Supporting Information of

Oxidative Dehydrogenation of Propane on the Oxygen Adsorbed Edges of Boron Nitride Nanoribbons

Biplab Rajbanshi,[†] Supriya Saha,[‡] Charles Fricke,[†] Salai Cheettu Ammal,[†] and Andreas Heyden*,[†]

Department of Chemical Engineering, University of South Carolina, 301 South Main Street, Columbia, South Carolina 29208, USA

CSIR-North East Institute of Science and Technology, Jorhat, Assam 785006, India.

E-mail: heyden@cec.sc.edu

*To whom correspondence should be addressed

[†]Department of Chemical Engineering, University of South Carolina

[‡]CSIR-North East Institute of Science and Technology

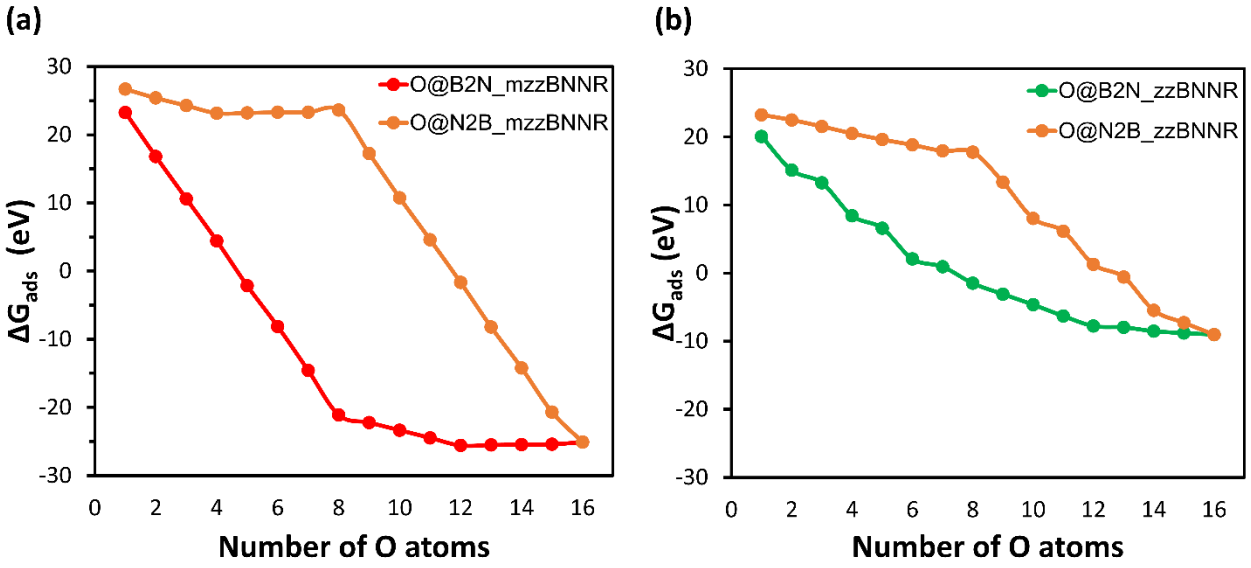

Figure S1: Gibbs free energy (ΔG_{ads}) variation with O adsorption starting from B-edge (O@B2N) and N-edge (O@N2B) of (a) mzzBNNR and (b) zzBNNR. Color codes are shown in the corresponding inset and consistent with Figure 2 of the main manuscript. All energies are with reference to the sum of the energies of the optimized supercell of bare armBNNR and molecular oxygen (T = 800 K and P_{O_2} = 0.15 atm).

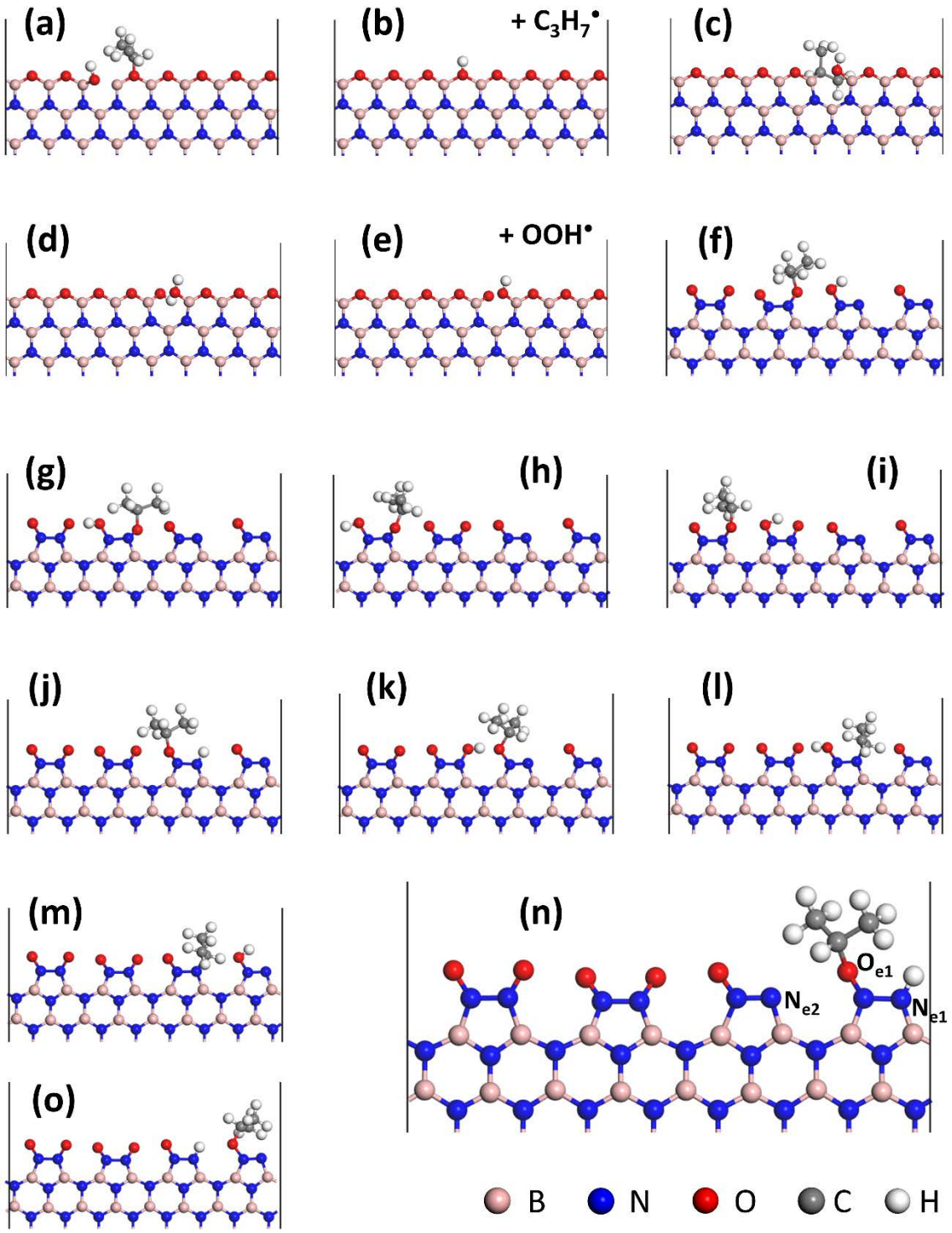

Figure S2: Relaxed structures of different possible configurations after first C-H cleavage of C_3H_8 on different sites of BNNR14O edges: (a) P1 (b) P2 (c) P3 (d) P4 (e) P5 (f) P6 (g) P7 (h) P8 (i) P9 (j) P10 (k) P11 (l) P12 (m) P13 (n) P14 (o) P15. (a)-(e) are structures on the B-edge, while all others are on the N-edge. The edge N and O atoms involved in H abstraction from C_3H_8 are denoted in the inset of the most stable intermediate P14 (n). Color code of the atoms is shown in the inset.

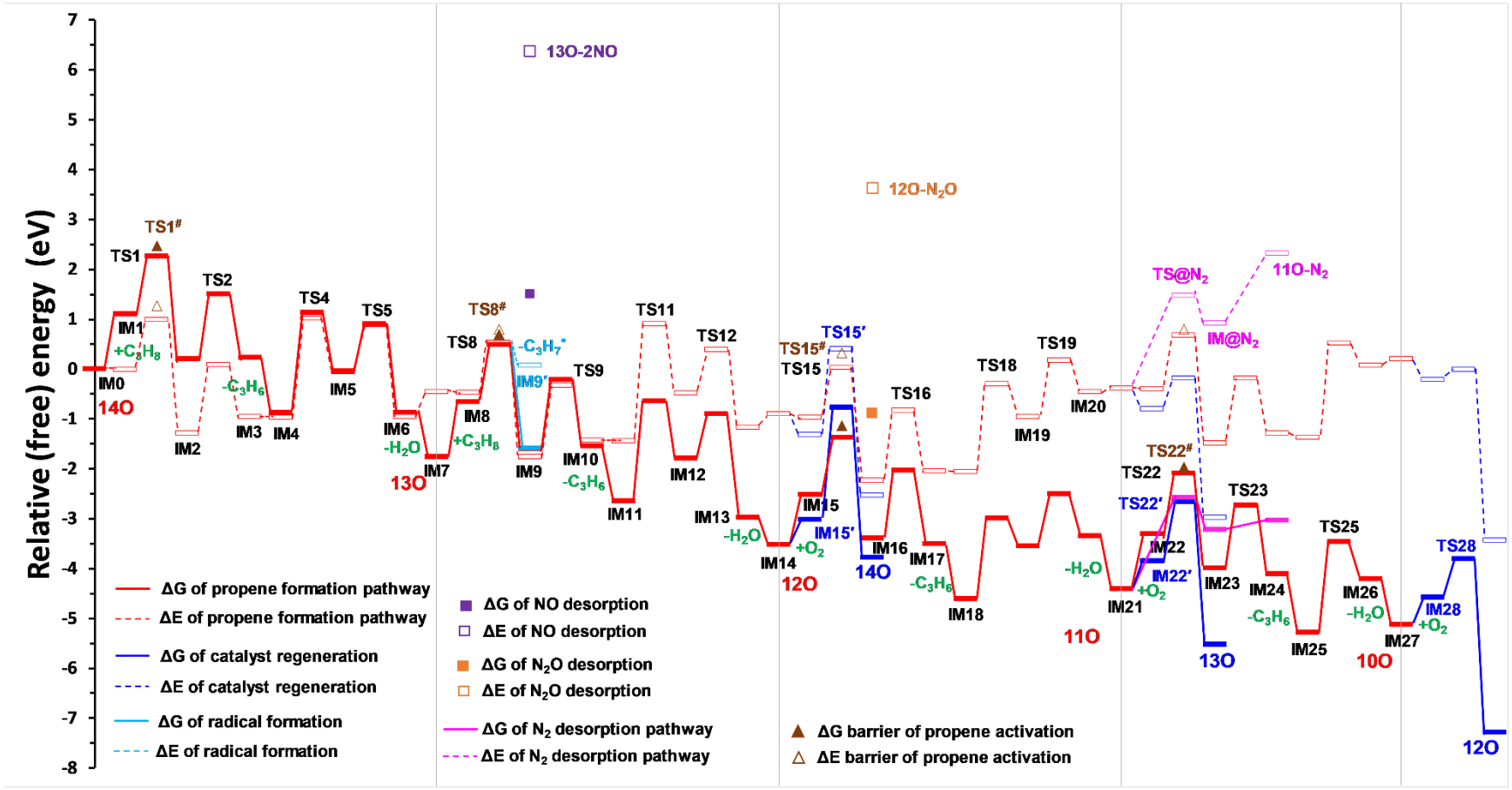

Figure S3: Free energy and zero-point energy (ZPE) corrected energy profiles for ODHP reaction on the O@mzzBNNR catalyst, denoted by solid and dashed lines, respectively. All free energies are calculated with reference to the sum of the energies of BNNR14O and the reactant gas molecules. Color code of the pathways is shown in the inset. T = 800 K, $P_{C_3H_8}$ = 0.3 atm, P_{O_2} = 0.15 atm, $P_{C_3H_6}$ = 0.3 atm, $P_{C_3H_7^\bullet}$ = 0.3 atm, P_{N_2} = 0.55 atm, P_{N_2O} = 0.001 atm, and P_{NO} = 0.001 atm. Relative free energies and ZPE corrected energies of the propene activation barriers (TS1$^{\#}$, TS8$^{\#}$, TS15$^{\#}$ and TS22$^{\#}$), $C_3H_7^\bullet$ radical formation (IM9′), NO desorption (13O-2NO), N_2O desorption (12O-N_2O), and N_2 desorption pathway (TS@N_2, IM@N_2 and 11O-N_2) processes, of this figure and Figure 4 of the main manuscript, which are not included and corresponding processes, for comparison, which are included in the microkinetic model are tabulated in Table S2 of Supporting Information.

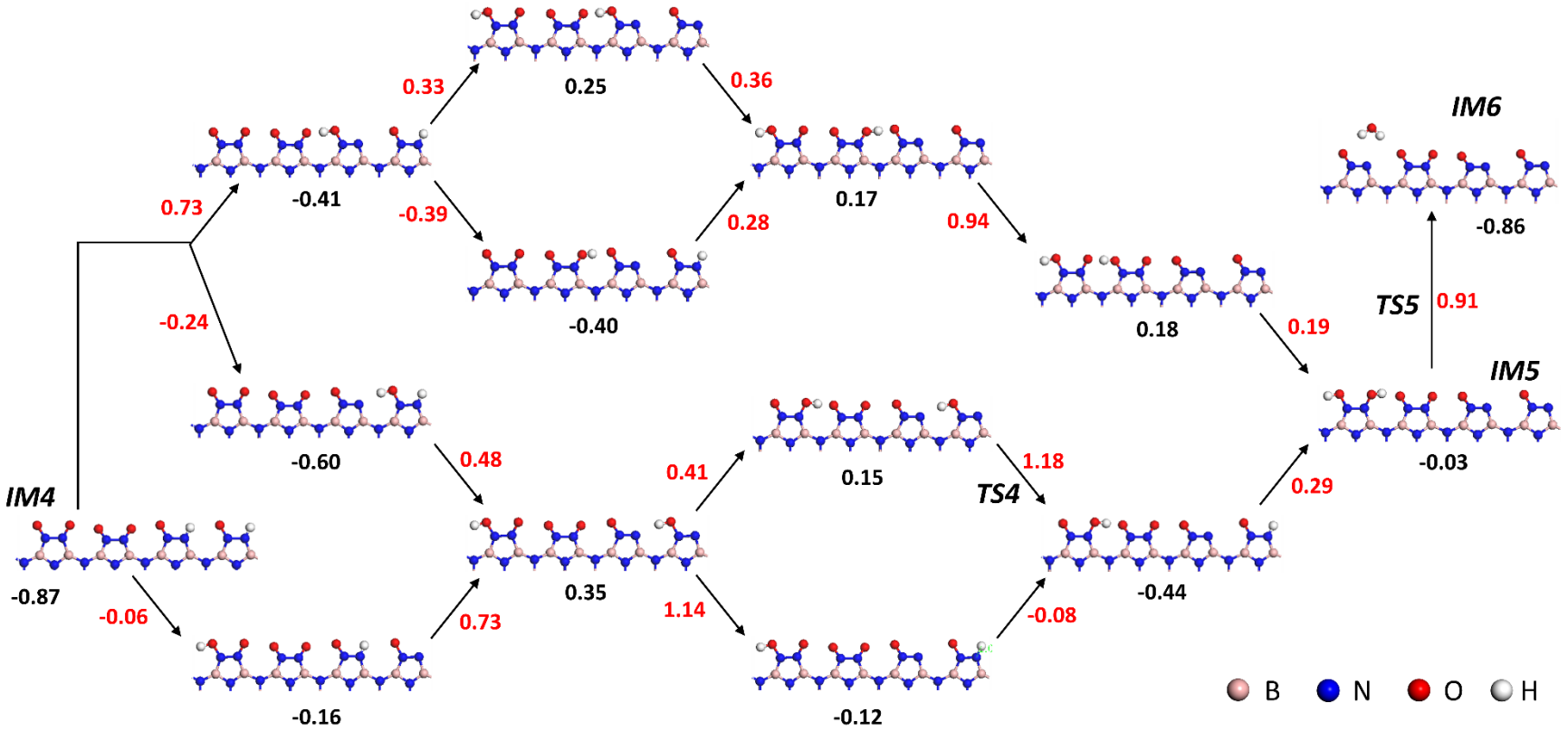

Figure S4: Possible H atom rearrangement pathways, from IM4 to IM6 of Figure 4, along with the optimized structures of the intermediates, and corresponding relative free energies (T = 800 K, $P_{C_3H_8}$ = 0.3 atm, and P_{O_2} = 0.15 atm) of the intermediates (black) and TSs (red), respectively. All free energies are calculated with reference to the sum of the energies of BNNR14O and the reactant gas molecules, C_3H_8 and O_2. Color code of the atoms is shown in the inset.

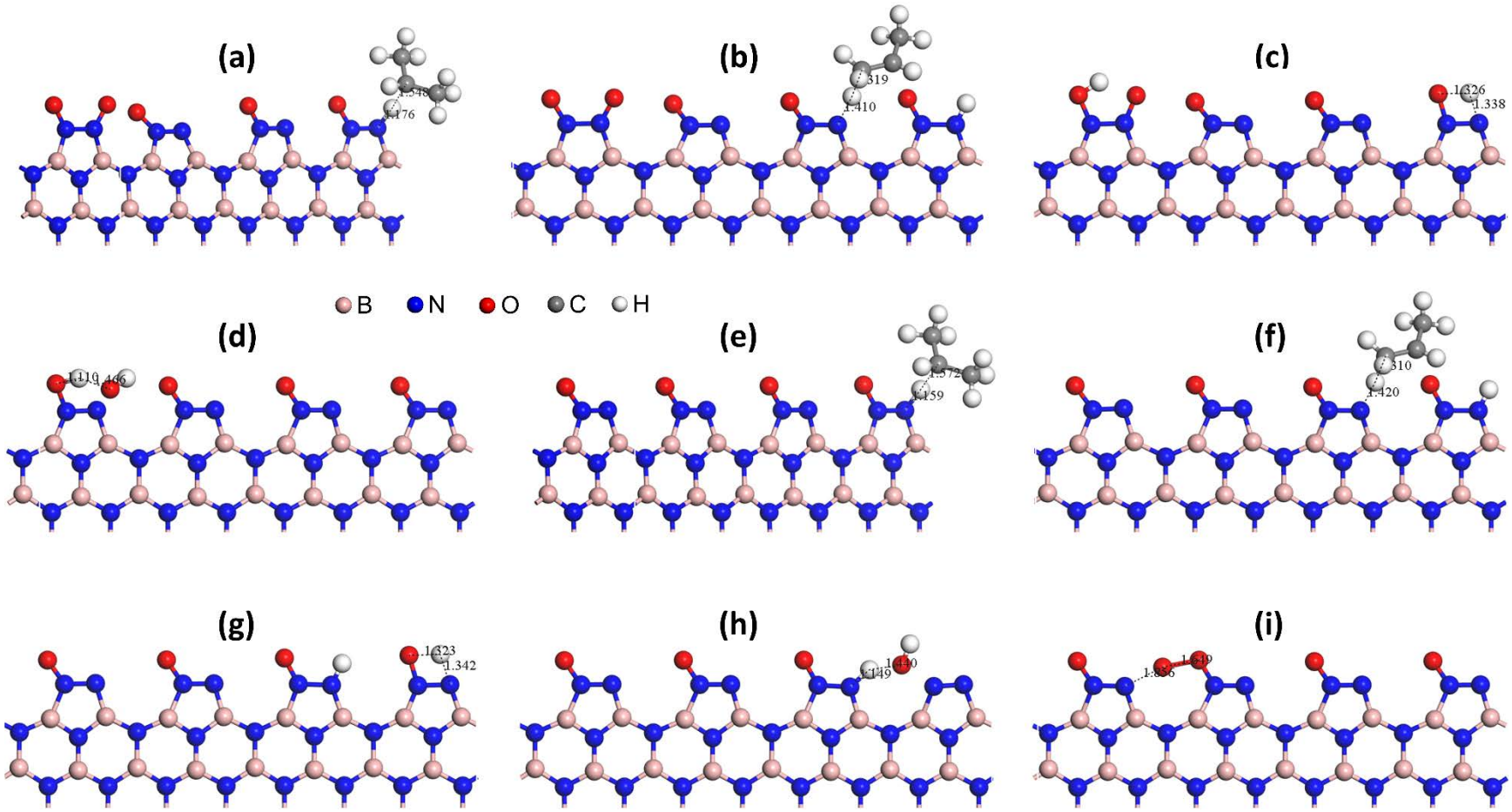

Figure S5: Relaxed structures of TSs involved along the most crucial 13O→11O→13O reaction cycle (Figure 5 of main manuscript): (a) TS8 (b) TS9 (c) TS11 (d) TS12 (e) TS15 (f) TS16 (g) TS18 (h) TS19 (i) TS22′. Color code of the atoms is shown in the inset.

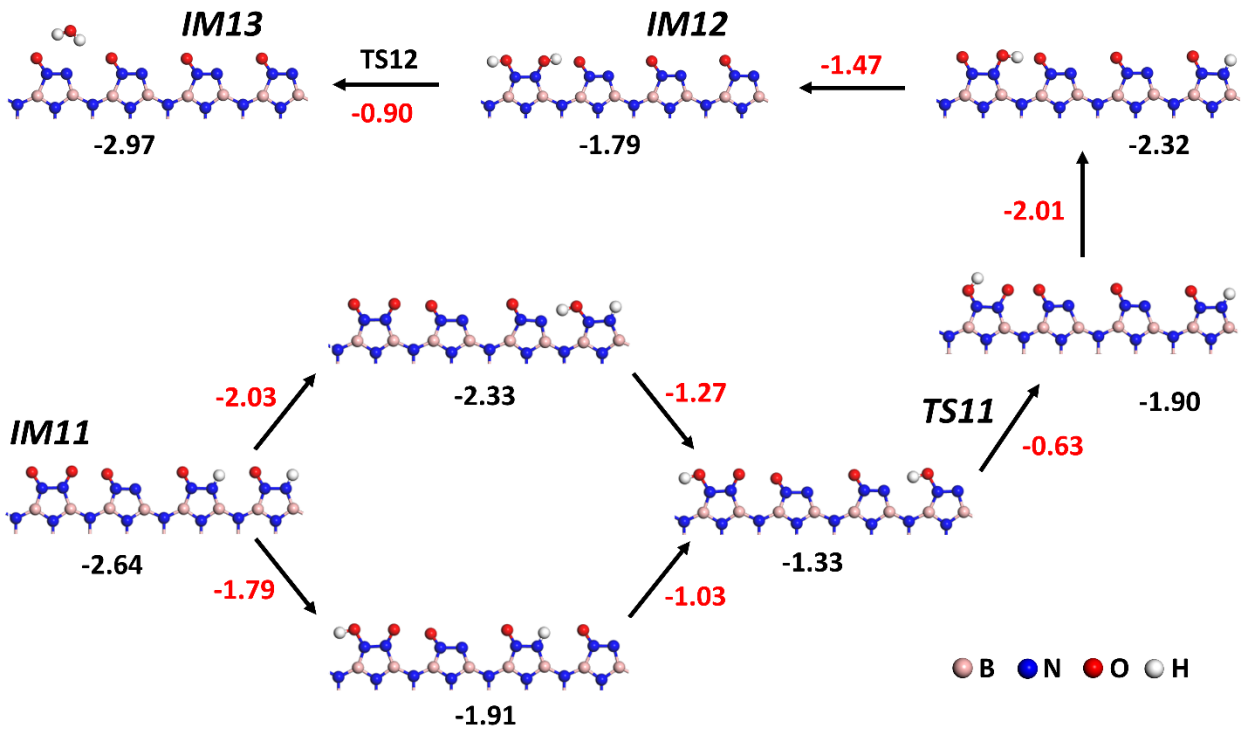

Figure S6: Possible H atom rearrangement pathways, from IM11 to IM13 of Figure 5, along with the optimized structures of intermediates and corresponding relative free energies (T = 800 K, $P_{C_3H_8}$ = 0.3 atm, and P_{O_2} = 0.15 atm) of the intermediates (black) and TSs (red), respectively. All free energies are calculated with reference to the sum of the energies of BNNR14O and the reactant gas molecules, C_3H_8 and O_2. Color code of the atoms is shown in the inset.

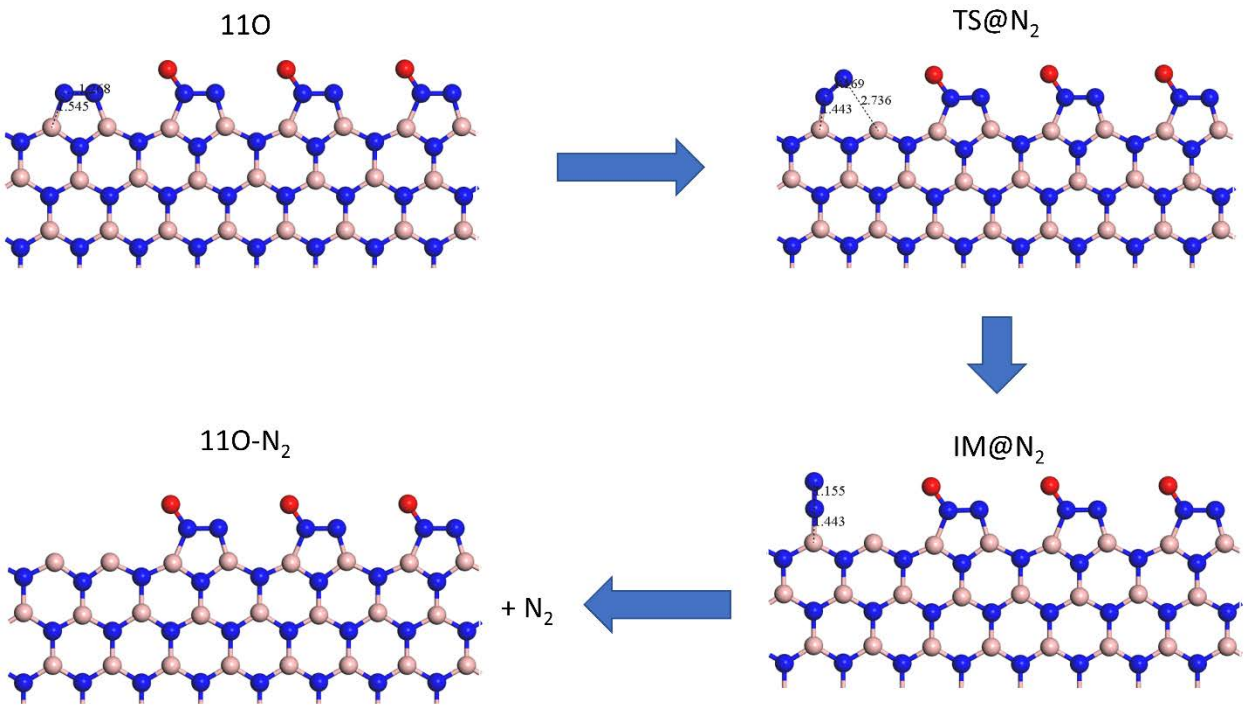

Figure S7: Relaxed structures of intermediates and transition state structures involved in the N_2 desorption pathway from 11O.

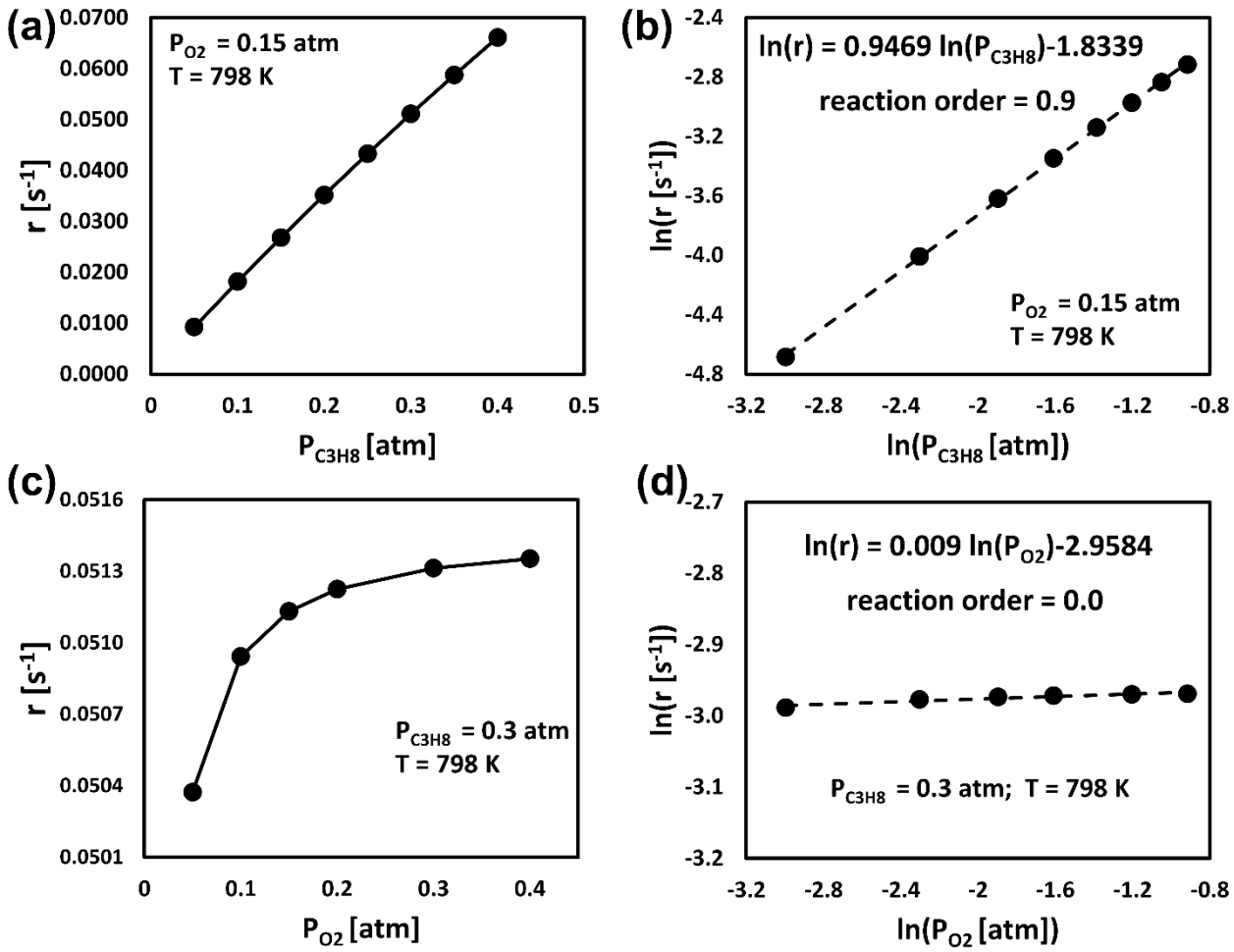

Figure S8: Effect of partial pressure of (a and b) C_3H_8 and (c and d) O_2 on the reaction rate (r [s^{-1}]) of the overall reaction, respectively, at T = 798 K.

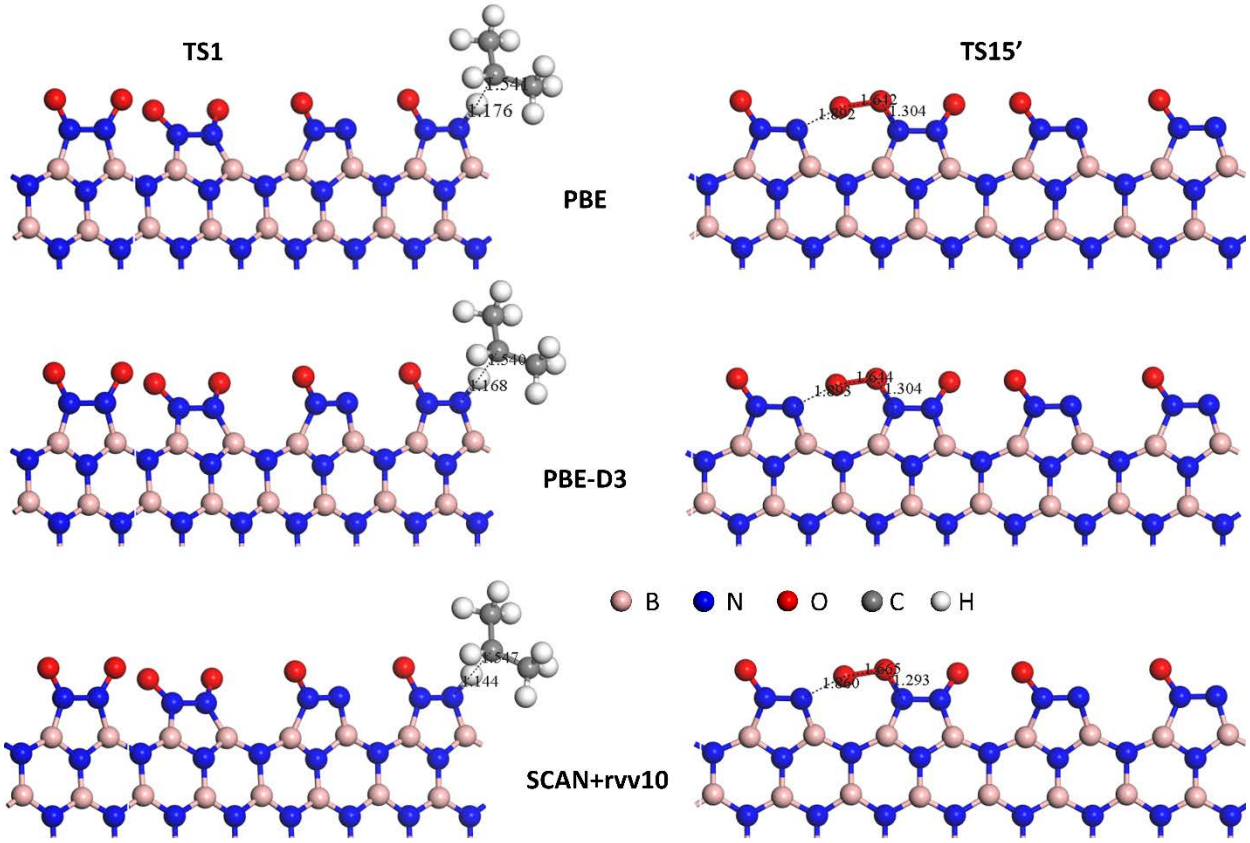

Figure S9: Transition state structures involved in the propane activation on BNNR14O (TS1) and O_2 dissociation over BNNR12O (TS15′) calculated using PBE (top), PBE-D3 (middle), and SCAN+rvv10 (bottom) functionals.

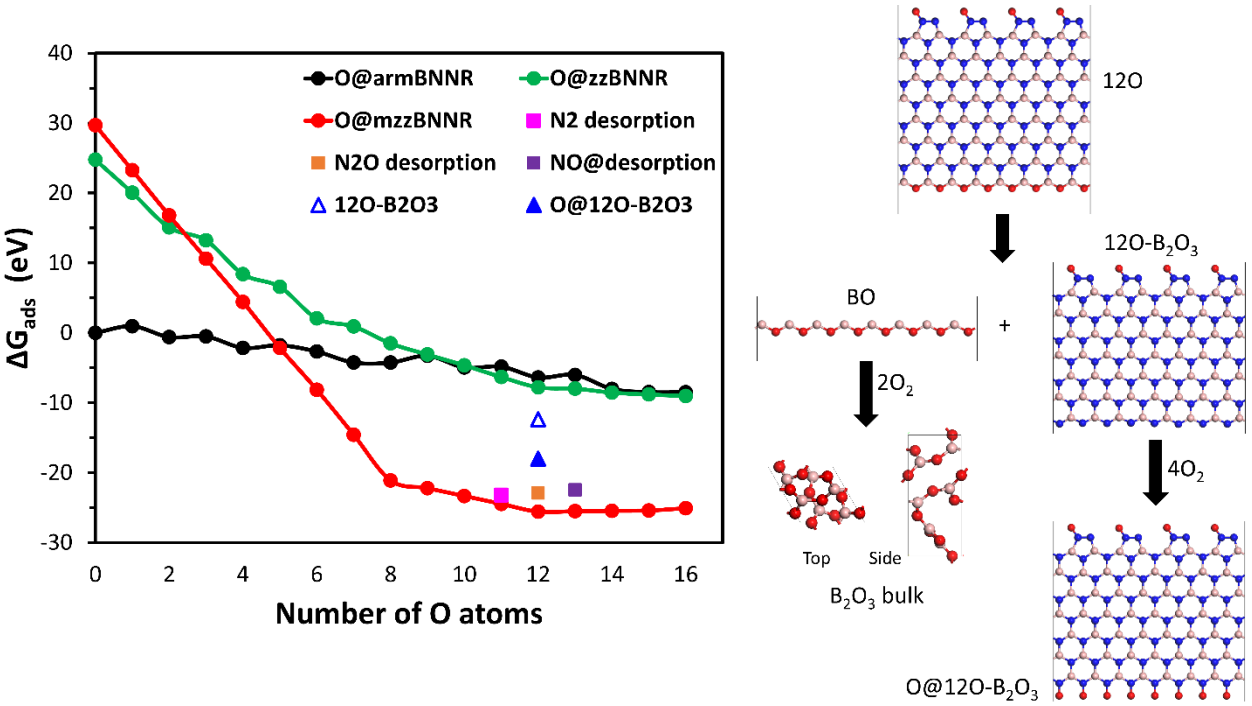

Figure S10: Gibbs free energy (ΔG_{ads}) of B loss from BNNR12O (shown in blue triangles) compared with the free energy of O passivation on the edges of the three BNNRs and N_2, NO and N_2O desorption from the considered catalysts. Color codes are shown in the corresponding inset. All free energies are calculated with reference to the energy of the optimized supercell of bare armchair BNNR at T = 800 K and P_{O_2} = 0.15 atm. P_{N_2} = 0.55 atm, P_{N_2O} = 0.001 atm, and P_{NO} = 0.001 atm. The optimized structures of the 1D BO, the nanoribbon after BO removal (12O-B_2O_3), the fully oxygen passivated nanoribbon after BO removal (O@12O-B_2O_3), and the unit-cell of bulk B_2O_3 are also shown on the right. One unit-cell of bulk B_2O_3 is composed of 6 B and 9 O atoms. Thus, to get the free energy for one-unit B_2O_3 we divided the energy of the bulk B_2O_3 unit-cell by 3. On the other hand, the one-dimensional BO precursor has 8 B and 8 O atoms. In the free energy calculation, we consider the energy of the precursor as $8BO = 4B_2O_3\text{-}2O_2$.

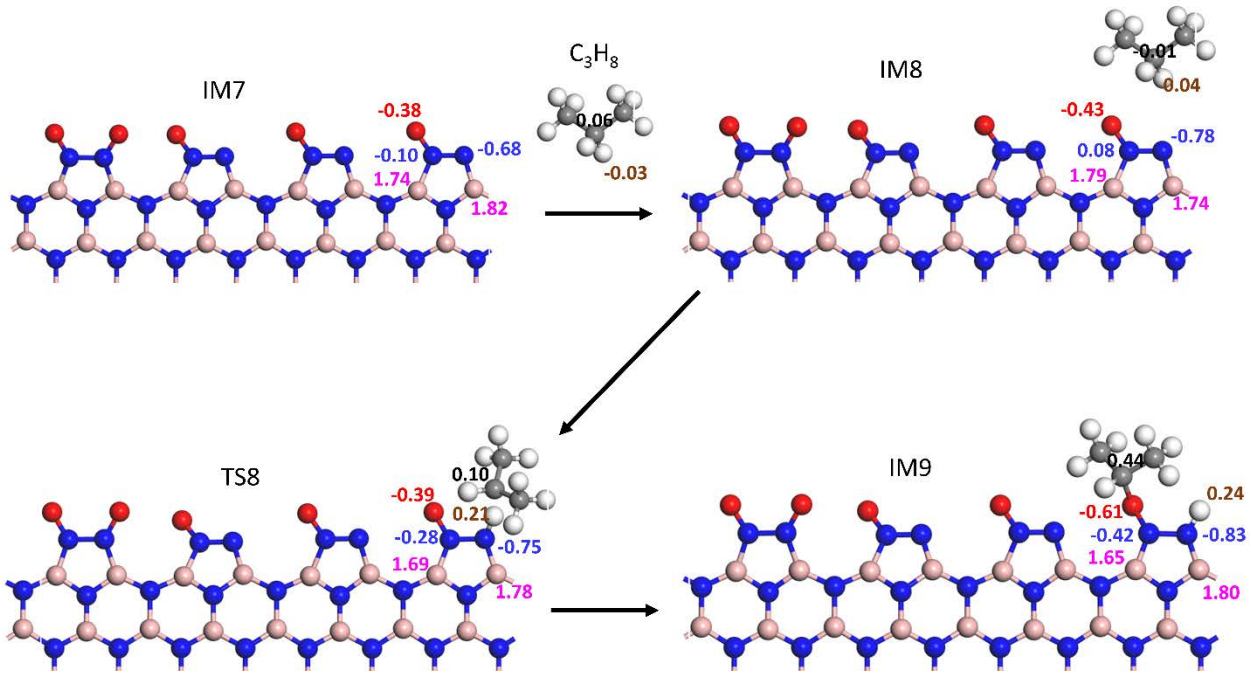

Figure S11: Calculated Bader charge of the edge atoms of the five-membered ring and the reactant propane for IM7, IM8, TS8, and IM9 of the proposed reaction mechanism for the ODHP.

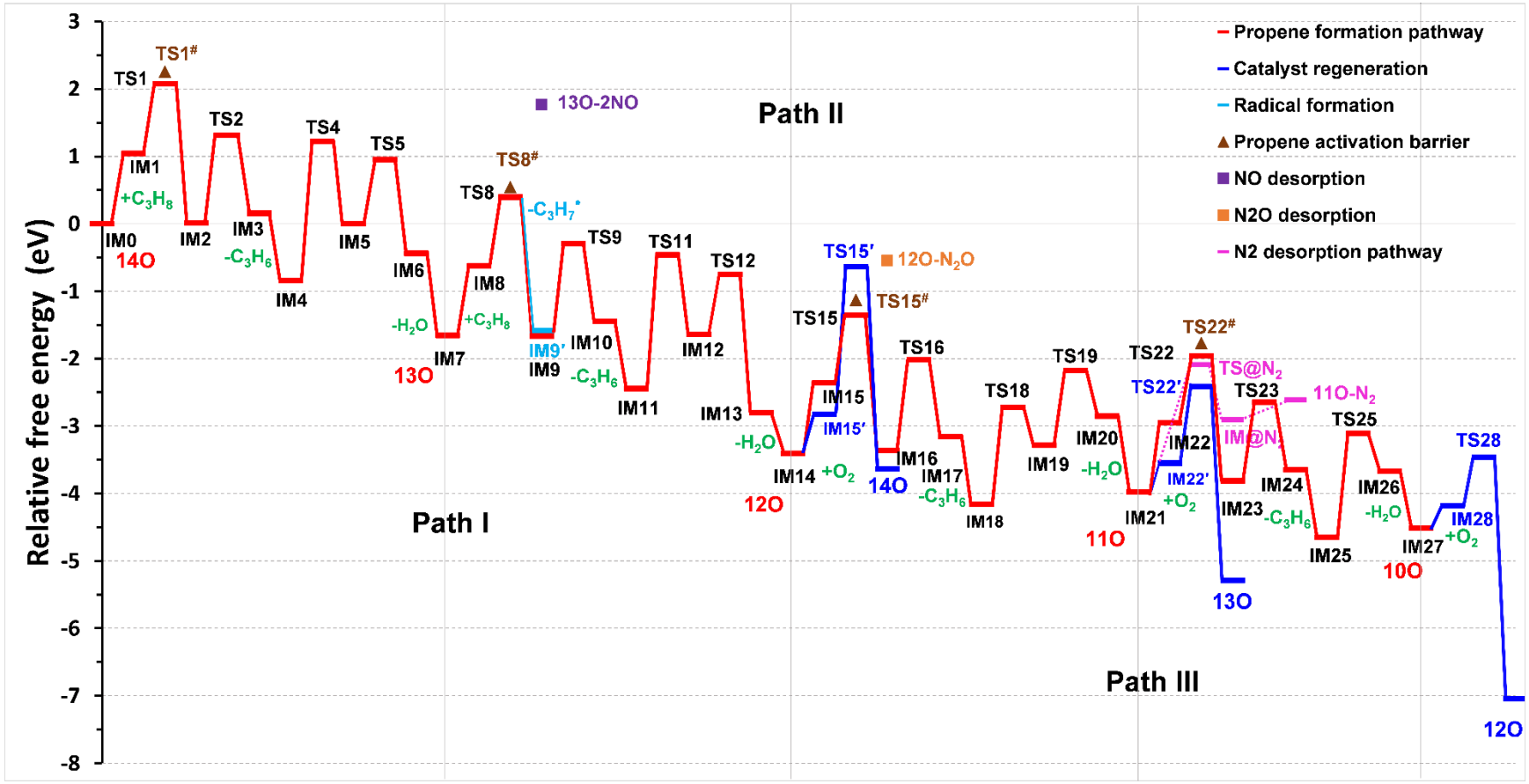

Figure S12: Free energy profiles for three different (coupled) catalytic cycles (Path I: 14O to 12O; Path II: 13O to 11O; and Path III: 12O to 10O) of the ODHP reaction on the O@mzzBNNR catalysts form single point PBE-D3 calculations. The color code of the different parts of the pathways are shown in the inset. All free energies are calculated with reference to the sum of the energies of BNNR14O and the reactant gas molecules, at T = 800 K, $P_{C_3H_8}$ = 0.3 atm, P_{O_2} = 0.15 atm, $P_{C_3H_6}$ = 0.3 atm, $P_{C_3H_7^\bullet}$ = 0.3 atm, P_{N_2} = 0.55 atm, P_{N_2O} = 0.001 atm, and P_{NO} = 0.001 atm.

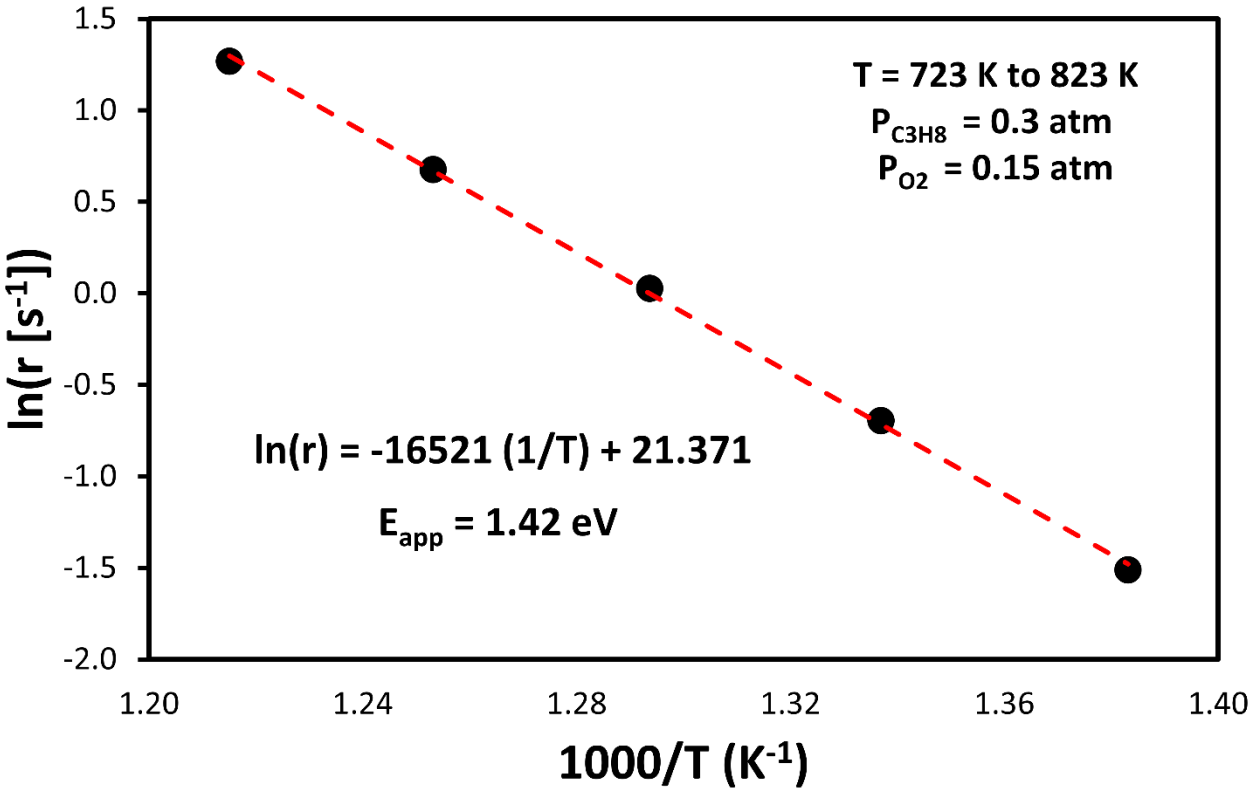

Figure S13: Arrhenius plot for the overall reaction based on energies computed using the PBE-D3 functional, revealing an apparent activation energy of 1.42 eV in a temperature range of 723 to 823 K, and $P_{C_3H_8}$ = 0.3 atm, P_{O_2} = 0.15 atm.

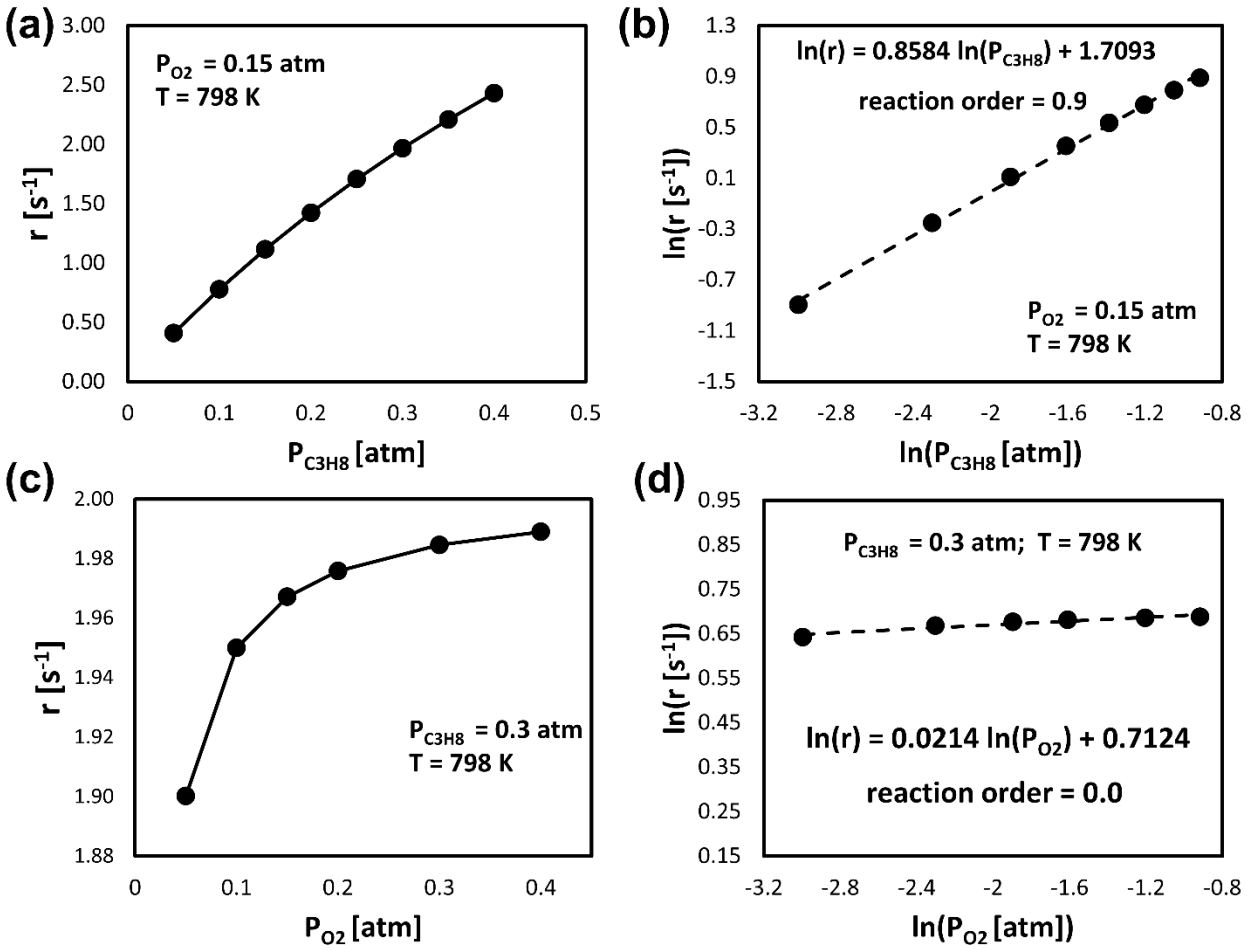

Figure S14: Effect of partial pressure of (a and b) C_3H_8 and (c and d) O_2 on the reaction rate (r [s^{-1}]) of the overall reaction, respectively, at T = 798 K. Data are based on a microkinetic model based on PBE-D3 single point calculations.

Table S1: Calculated relative free energies and ZPE corrected energies of different possible configurations (P1 to P15) after first C-H cleavage of C_3H_8 on different sites of the BNNR14O edge. All energies are referenced to the sum of the energies of BNNR14O and a gas phase C_3H_8 molecule. Free energies are computed at T= 800 K, $P_{C_3H_8}$ = 0.3 atm, P_{H_2O} = 0.3 atm, P_{O_2} = 0.15 atm, and $P_{O_2H\bullet}$ = 0.15 atm.

Possible intermediate structures	**P1**	**P2**	**P3**	**P4**	**P5**	**P6**
ΔG (eV)	7.21	4.18	2.58	1.17	3.08	1.50
ΔE (eV)	5.73	4.63	1.19	-0.17	1.96	0.06
Possible intermediate structures	**P7**	**P8**	**P9**	**P10**	**P11**	**P12**
ΔG (eV)	0.89	1.10	1.44	0.24	1.37	0.26
ΔE (eV)	-0.61	-0.40	-0.09	-1.24	-0.14	-1.23
Possible intermediate structures	**P13**	**P14**	**P15**			
ΔG (eV)	1.05	0.20	0.82			
ΔE (eV)	-0.51	-1.28	-0.61			

Table S2: Relative free energies (**ΔG**) and ZPE corrected energies ($\Delta \boldsymbol{E_{ZPE}}$) of the propene activation barriers (TS1$^{\#}$, TS8$^{\#}$, TS15$^{\#}$ and TS22$^{\#}$), $C_3H_7^{\bullet}$ radical formation (IM9′), NO desorption (13O-2NO), N_2O desorption (12O-N_2O), and N_2 desorption pathway (TS@N_2, IM@N_2 and 11O-N_2) as shown in Figure 4 of the main manuscript and Figure S3 of Supporting Information. These pathways are not included in the microkinetic model considered in the present work. For comparison, the ΔG and $\Delta \boldsymbol{E_{ZPE}}$ of corresponding important states, which are included in the microkinetic model, are also tabulated. All free energies are calculated with reference to the sum of the energies of BNNR14O and the reactant gas molecules at T = 800 K, $P_{C_3H_8}$ = 0.3 atm, P_{O_2} = 0.15 atm, $P_{C_3H_6}$ = 0.3 atm, $P_{C_3H_7^{\bullet}}$ = 0.3 atm, P_{N_2} = 0.55 atm, P_{N_2O} = 0.001 atm, and P_{NO} = 0.001 atm.

Structures	**ΔG (eV)**	**ΔE_{ZPE} (eV)**
BNNR14O (IM0)	0.00	0.00
TS1	2.27	0.99
TS1$^{\#}$	2.47	1.26
BNNR13O (IM7)	-1.75	-0.45
TS8	0.49	0.54
TS8$^{\#}$	0.69	0.79
IM9	-1.60	-1.76
IM9′	-1.58	0.07
13O-2NO	1.49	6.37
BNNR12O (IM14)	-3.52	-0.90
TS15	-1.37	0.03
TS8$^{\#}$	-1.14	0.32
12O-N_2O	-0.89	3.61
BNNR11O (IM21)	-4.40	-0.39
TS22	-2.08	0.68
TS22$^{\#}$	-1.98	0.79
TS22′	-2.66	-0.18
TS@N_2	-2.57	1.48
IM@N_2	-3.22	0.92
11O-N_2	-3.03	2.32

Table S3: ZPE corrected reaction energies (ΔE_{ZPE}^{rxn}), forward activation barriers (ΔE_{ZPE}^{act}), and calculated imaginary vibrational frequencies for the corresponding transition state of the elementary steps considered in the overall reaction network of the ODHP reaction.

Reaction	ΔE_{ZPE}^{rxn} (eV)	ΔE_{ZPE}^{act} (eV)	Frequency (i) (cm^{-1})
(R1) BNNR14O (IM0) + $C_3H_{8\,(g)}$ → BNNR14O-C_3H_8 (IM1)	-0.01	-	
(R2) BNNR14O-C_3H_8 (IM1) → BNNR14O-C_3H_7-H (IM2)	-1.27	1.00	987
(R3) BNNR14O-C_3H_7-H (IM2) → BNNR14O-2H-C_3H_6 (IM3)	0.33	1.37	1184
(R4) BNNR14O-2H-C_3H_6 (IM3) → BNNR14O-2H (IM4) + $C_3H_{6\,(g)}$	-0.01	-	
(R5) BNNR14O-2H (IM4) → BNNR14O-2Hr (IM5)	0.92	1.99	1736
(R6) BNNR14O-2Hr (IM5) → BNNR13O-H_2O (IM6)	-0.90	0.95	722
(R7) BNNR13O-H_2O (IM6) → BNNR13O (IM7) + $H_2O_{\,(g)}$	0.50	-	
(R8) BNNR13O (IM7) + $C_3H_{8\,(g)}$ → BNNR13O-C_3H_8 (IM8)	-0.02	-	
(R9) BNNR13O-C_3H_8 (IM8) → BNNR13O-C_3H_7-H (IM9)	-1.29	1.00	992
(R10) BNNR13O-C_3H_7-H (IM9) → BNNR13O-2H-C_3H_6 (IM10)	0.34	1.44	1255
(R11) BNNR13O-2H-C_3H_6 (IM10) → BNNR13O-2H (IM11) + $C_3H_{6\,(g)}$	-0.02	-	
(R12) BNNR13O-2H (IM11) → BNNR13O-2Hr (IM12)	0.95	2.01	1736
(R13) BNNR13O-2Hr (IM12) → BNNR12O-H_2O (IM13)	-0.68	0.89	674
(R14) BNNR12O-H_2O (IM13) → BNNR12O (IM14) + $H_2O_{\,(g)}$	0.20	-	
(R15) BNNR12O (IM14) + $C_3H_{8\,(g)}$ → BNNR12O- C_3H_8 (IM15)	-0.01	-	
(R16) BNNR12O-C_3H_8 (IM15) → BNNR12O-C_3H_7-H (IM16)	-1.25	1.00	857
(R17) BNNR12O-C_3H_7-H (IM16) → BNNR12O-2H-C_3H_6 (IM17)	0.19	1.41	1399
(R18) BNNR12O-2H-C_3H_6 (IM17) → BNNR12O-2H (IM18) + $C_3H_{6\,(g)}$	-0.02	-	
(R19) BNNR12O-2H (IM18) → BNNR12O-2Hr (IM19)	1.11	1.88	1721
(R20) BNNR12O-2Hr (IM19) → BNNR11O-H_2O (IM20)	0.50	1.13	2105
(R21) BNNR11O-H_2O (IM20) → BNNR11O (IM21) + $H_2O_{\,(g)}$	0.06	-	
(R22) BNNR11O (IM21) + $O_{2\,(g)}$ → BNNR11O-O_2 (IM22′)	-0.41	-	
(R23) BNNR11O-O_2 (IM22′) → BNNR13O (IM7)	-2.18	0.62	526
(R24) BNNR11O (IM21) + $C_3H_{8\,(g)}$ → BNNR11O- C_3H_8 (IM22)	-0.01	-	
(R25) BNNR11O-C_3H_8 (IM22) → BNNR11O-C_3H_7-H (IM23)	-1.08	1.07	844
(R26) BNNR11O-C_3H_7-H (IM23) → BNNR11O-2H-C_3H_6 (IM24)	0.20	1.30	1338
(R27) BNNR11O-2H-C_3H_6 (IM24) → BNNR11O-2H (IM25) + $C_3H_{6\,(g)}$	-0.09	-	
(R28) BNNR11O-2H (IM25) → BNNR10O-H_2O (IM26)	1.44	1.90	890
(R29) BNNR10O-H_2O (IM26) → BNNR10O (IM27) + $H_2O_{\,(g)}$	0.13	-	
(R30) BNNR10O (IM27) + $O_{2\,(g)}$ → BNNR10O-O_2 (IM28)	-0.41	-	

(R31) BNNR10O-O_2 (IM28) → BNNR12O (IM14)	-3.28	0.19	513
(R32) BNNR12O (IM14) + $O_{2\,(g)}$ → BNNR12O-O_2 (IM15′)	-0.44	-	
(R33) BNNR12O-O_2 (IM15′) → BNNR14O (IM0)	-1.11	1.82	470

Table S4: Forward rate constants (k_{for}) and equilibrium constants (K) calculated at different temperatures for the elementary steps considered in overall reaction network of the ODHP reaction ($P_{C_3H_8}$ = 0.3 atm and P_{O_2} = 0.15 atm).

Reaction	T= 748 K		T = 798 K		T = 823 K	
	k_{for} (s^{-1})	K	k_{for} (s^{-1})	K	k_{for} (s^{-1})	K
R1	3.03×10^{9}	9.36×10^{-8}	2.94×10^{9}	1.04×10^{-7}	2.89×10^{9}	1.09×10^{-7}
R2	2.94×10^{5}	1.99×10^{6}	8.17×10^{5}	5.52×10^{5}	1.30×10^{6}	3.08×10^{5}
R3	2.13×10^{4}	4.20×10^{-1}	8.81×10^{4}	6.22×10^{-1}	1.68×10^{5}	7.44×10^{-1}
R4	2.75×10^{16}	8.87×10^{6}	2.38×10^{16}	7.93×10^{6}	2.24×10^{16}	7.57×10^{6}
R5	5.08×10^{-1}	2.28×10^{-6}	3.61	5.55×10^{-6}	8.81	8.31×10^{-6}
R6	1.82×10^{6}	4.09×10^{5}	4.70×10^{6}	1.69×10^{5}	7.25×10^{6}	1.13×10^{5}
R7	1.03×10^{15}	2.18×10^{5}	1.65×10^{15}	3.60×10^{5}	2.06×10^{15}	4.55×10^{5}
R8	3.03×10^{9}	1.01×10^{-7}	2.94×10^{9}	1.13×10^{-7}	2.89×10^{9}	1.17×10^{-7}
R9	3.74×10^{5}	3.68×10^{6}	1.04×10^{6}	1.00×10^{6}	1.66×10^{6}	5.54×10^{5}
R10	5.84×10^{3}	2.75×10^{-1}	2.59×10^{4}	4.10×10^{-1}	5.10×10^{4}	4.93×10^{-1}
R11	3.41×10^{16}	1.10×10^{7}	2.95×10^{16}	9.82×10^{6}	2.77×10^{16}	9.36×10^{6}
R12	4.03×10^{-1}	5.60×10^{-7}	2.92	1.40×10^{-6}	7.17	2.13×10^{-6}
R13	7.12×10^{7}	1.17×10^{8}	1.82×10^{8}	6.75×10^{7}	2.80×10^{8}	5.26×10^{7}
R14	4.82×10^{13}	1.02×10^{4}	5.15×10^{13}	1.12×10^{4}	5.34×10^{13}	1.18×10^{4}
R15	3.03×10^{9}	9.18×10^{-8}	2.94×10^{9}	1.03×10^{-7}	2.89×10^{9}	1.07×10^{-7}
R16	3.80×10^{5}	1.24×10^{6}	1.06×10^{6}	3.52×10^{5}	1.69×10^{6}	1.98×10^{5}
R17	1.09×10^{4}	3.86	4.68×10^{4}	5.02	9.10×10^{4}	5.66
R18	3.13×10^{16}	1.01×10^{7}	2.69×10^{16}	8.96×10^{6}	2.52×10^{16}	8.53×10^{6}
R19	5.98	6.43×10^{-8}	4.01×10^{1}	1.90×10^{-7}	9.52×10^{1}	3.11×10^{-7}
R20	1.28×10^{6}	2.84×10^{-2}	4.07×10^{6}	4.94×10^{-2}	6.89×10^{6}	6.36×10^{-2}
R21	2.00×10^{16}	4.22×10^{6}	1.96×10^{16}	4.26×10^{6}	1.95×10^{16}	4.32×10^{6}
R22	1.78×10^{9}	4.37×10^{-4}	1.72×10^{9}	3.20×10^{-4}	1.69×10^{9}	2.77×10^{-4}
R23	3.20×10^{5}	3.68×10^{11}	5.52×10^{5}	4.07×10^{10}	7.07×10^{5}	1.49×10^{10}
R24	3.03×10^{9}	1.18×10^{-7}	2.94×10^{9}	1.32×10^{-7}	2.89×10^{9}	1.38×10^{-7}

R25	9.59×10^{4}	6.42×10^{4}	2.84×10^{5}	2.14×10^{4}	4.67×10^{5}	1.29×10^{4}
R26	4.30×10^{4}	3.77	1.67×10^{5}	4.96	3.11×10^{5}	5.62
R27	8.97×10^{16}	2.89×10^{7}	7.21×10^{16}	2.40×10^{7}	6.54×10^{16}	2.21×10^{7}
R28	7.19	3.24×10^{-8}	4.88×10^{1}	1.43×10^{-7}	1.17×10^{2}	2.81×10^{-7}
R29	2.45×10^{15}	5.16×10^{5}	2.53×10^{15}	5.51×10^{5}	2.59×10^{15}	5.73×10^{5}
R30	1.78×10^{9}	5.58×10^{-4}	1.72×10^{9}	4.10×10^{-4}	1.69×10^{9}	3.56×10^{-4}
R31	2.05×10^{8}	1.56×10^{19}	2.31×10^{8}	5.77×10^{17}	2.44×10^{8}	1.29×10^{17}
R32	1.78×10^{9}	8.16×10^{-4}	1.72×10^{9}	5.77×10^{-4}	1.69×10^{9}	4.92×10^{-4}
R33	4.80×10^{-3}	4.77×10^{4}	2.73×10^{-2}	1.53×10^{4}	6.01×10^{-2}	9.13×10^{3}

Table S5: Surface coverage/probability density (θ) of various intermediates calculated at different temperatures for overall pathway of the ODHP reaction (P_{C3H8}= 0.3, and P_{O2}= 0.15 atm).

Intermediate		Surface Coverage (θ)		
		748 K	798 K	823 K
BNNR14O	(IM0)	5.12×10^{-5}	7.35×10^{-5}	1.07×10^{-4}
BNNR14O-C_3H_8	(IM1)	4.79×10^{-12}	7.66×10^{-12}	1.16×10^{-11}
BNNR14O-C_3H_7-H	(IM2)	6.77×10^{-11}	7.17×10^{-11}	9.05×10^{-11}
BNNR14O-2H-C_3H_6	(IM3)	5.58×10^{-13}	4.09×10^{-13}	4.00×10^{-13}
BNNR14O-2H	(IM4)	4.95×10^{-6}	3.24×10^{-6}	3.03×10^{-6}
BNNR14O-2Hr	(IM5)	4.96×10^{-12}	8.48×10^{-12}	1.09×10^{-11}
BNNR13O-H_2O	(IM6)	1.71×10^{-6}	1.21×10^{-6}	9.91×10^{-7}
BNNR13O	(IM7)	3.72×10^{-1}	4.35×10^{-1}	4.51×10^{-1}
BNNR13O-C_3H_8	(IM8)	3.77×10^{-8}	4.90×10^{-8}	5.29×10^{-8}
BNNR13O-C_3H_7-H	(IM9)	2.43×10^{-6}	1.98×10^{-6}	1.73×10^{-6}
BNNR13O-2H-C_3H_6	(IM10)	3.22×10^{-9}	1.81×10^{-9}	1.33×10^{-9}
BNNR13O-2H	(IM11)	3.54×10^{-2}	1.77×10^{-2}	1.24×10^{-2}
BNNR13O-2Hr	(IM12)	1.99×10^{-10}	2.81×10^{-10}	3.16×10^{-10}
BNNR12O-H_2O	(IM13)	3.98×10^{-5}	4.21×10^{-5}	4.13×10^{-5}
BNNR12O	(IM14)	4.05×10^{-1}	4.72×10^{-1}	4.88×10^{-1}
BNNR12O-C_3H_8	(IM15)	3.72×10^{-8}	4.84×10^{-8}	5.22×10^{-8}
BNNR12O-C_3H_7-H	(IM16)	1.30×10^{-6}	1.09×10^{-6}	9.69×10^{-7}
BNNR12O-2H-C_3H_6	(IM17)	1.86×10^{-8}	8.32×10^{-9}	5.55×10^{-9}
BNNR12O-2H	(IM18)	1.87×10^{-1}	7.46×10^{-2}	4.73×10^{-2}
BNNR12O-2Hr	(IM19)	1.19×10^{-8}	1.39×10^{-8}	1.44×10^{-8}
BNNR11O-H_2O	(IM20)	2.39×10^{-11}	6.79×10^{-11}	1.04×10^{-10}
BNNR11O	(IM21)	1.01×10^{-4}	2.89×10^{-4}	4.49×10^{-4}
BNNR11O-O_2	(IM22′)	4.42×10^{-8}	9.26×10^{-8}	1.24×10^{-7}

BNNR11O-C_3H_8	(IM22)	1.19×10^{-11}	3.83×10^{-11}	6.20×10^{-11}
BNNR11O-C_3H_7-H	(IM23)	2.66×10^{-11}	6.51×10^{-11}	9.33×10^{-11}
BNNR11O-2H-C_3H_6	(IM24)	5.53×10^{-15}	9.36×10^{-15}	1.13×10^{-14}
BNNR11O-2H	(IM25)	1.60×10^{-7}	2.25×10^{-7}	2.50×10^{-7}
BNNR10O-H_2O	(IM26)	1.94×10^{-17}	2.08×10^{-16}	5.82×10^{-16}
BNNR10O	(IM27)	1.00×10^{-11}	1.15×10^{-10}	3.33×10^{-10}
BNNR10O-O_2	(IM28)	5.60×10^{-15}	4.71×10^{-14}	1.19×10^{-13}
BNNR12O-O_2	(IM15′)	3.30×10^{-4}	2.72×10^{-4}	2.40×10^{-4}

Table S6: Selected bond parameters and relative free energies of transition state structures involved in the propane activation on BNNR14O (TS1), O_2 dissociation over BNNR12O (TS15′), and the intermediate BNNR12O (IM14) calculated using the PBE, PBE-D3 and SCAN+rvv10 functionals. All structures are fully optimized with the corresponding DFT functional. All free energies are calculated with reference to the sum of the energies of BNNR14O and the reactant gas molecules, C_3H_8 and O_2. (T = 800 K, $P_{C_3H_8}$ = 0.3 atm, P_{O_2} = 0.15 atm).

	Bond lengths (Å)		**Relative free energy (eV)**		
	TS1	TS15′	TS1	IM14 (12O)	TS15′
PBE	C-H = 1.54 N-H = 1.18	N_r-O = 1.30 O-O = 1.64 N_l-O = 1.89	2.27	-3.52	-0.76
PBE-D3	C-H = 1.54 N-H = 1.17	N_r-O = 1.30 O-O = 1.64 N_l-O = 1.89	2.08	-3.41	-0.64
SCAN +rvv10	C-H = 1.55 N-H = 1.14	N_r-O = 1.29 O-O = 1.66 N_l-O = 1.86	2.44	-3.44	-0.57

Table S7: ZPE corrected reaction energies (ΔE_{ZPE}^{rxn}), forward activation barriers (ΔE_{ZPE}^{act}), and calculated imaginary vibrational frequency for the corresponding transition state of the elementary steps considered in the overall reaction network of the ODHP reaction. PBE energies are corrected by PBE-D3 single point calculations.

Reaction	ΔE_{ZPE}^{rxn} (eV)	ΔE_{ZPE}^{act} (eV)	Frequency (i) (cm^{-1})
(R1) BNNR14O (IM0) + $C_3H_{8\,(g)}$ → BNNR14O-C_3H_8 (IM1)	-0.14	-	
(R2) BNNR14O-C_3H_8 (IM1) → BNNR14O-C_3H_7-H (IM2)	-1.40	0.86	958
(R3) BNNR14O-C_3H_7-H (IM2) → BNNR14O-2H-C_3H_6 (IM3)	0.44	1.36	1181
(R4) BNNR14O-2H-C_3H_6 (IM3) → BNNR14O-2H (IM4) + $C_3H_{6\,(g)}$	0.09	-	
(R5) BNNR14O-2H (IM4) → BNNR14O-2Hr (IM5)	0.93	2.05	1738
(R6) BNNR14O-2Hr (IM5) → BNNR13O-H_2O (IM6)	-0.51	0.95	725
(R7) BNNR13O-H_2O (IM6) → BNNR13O (IM7) + $H_2O_{\,(g)}$	0.17	-	
(R8) BNNR13O (IM7) + $C_3H_{8\,(g)}$ → BNNR13O-C_3H_8 (IM8)	-0.14	-	
(R9) BNNR13O-C_3H_8 (IM8) → BNNR13O-C_3H_7-H (IM9)	-1.39	0.88	982
(R10) BNNR13O-C_3H_7-H (IM9) → BNNR13O-2H-C_3H_6 (IM10)	0.49	1.42	1259
(R11) BNNR13O-2H-C_3H_6 (IM10) → BNNR13O-2H (IM11) + $C_3H_{6\,(g)}$	0.09	-	
(R12) BNNR13O-2H (IM11) → BNNR13O-2Hr (IM12)	0.90	1.89	1731
(R13) BNNR13O-2Hr (IM12) → BNNR12O-H_2O (IM13)	-0.65	0.89	672
(R14) BNNR12O-H_2O (IM13) → BNNR12O (IM14) + $H_2O_{\,(g)}$	0.25	-	
(R15) BNNR12O (IM14) + $C_3H_{8\,(g)}$ → BNNR12O- C_3H_8 (IM15)	-0.14	-	
(R16) BNNR12O-C_3H_8 (IM15) → BNNR12O-C_3H_7-H (IM16)	-1.38	0.86	853
(R17) BNNR12O-C_3H_7-H (IM16) → BNNR12O-2H-C_3H_6 (IM17)	0.51	1.40	1394
(R18) BNNR12O-2H-C_3H_6 (IM17) → BNNR12O-2H (IM18) + $C_3H_{6\,(g)}$	0.09	-	
(R19) BNNR12O-2H (IM18) → BNNR12O-2Hr (IM19)	0.92	1.69	1721
(R20) BNNR12O-2Hr (IM19) → BNNR11O-H_2O (IM20)	0.72	1.09	2102
(R21) BNNR11O-H_2O (IM20) → BNNR11O (IM21) + $H_2O_{\,(g)}$	0.01	-	
(R22) BNNR11O (IM21) + $O_{2\,(g)}$ → BNNR11O-O_2 (IM22′)	-0.54	-	
(R23) BNNR11O-O_2 (IM22′) → BNNR13O (IM7)	-2.24	0.57	521
(R24) BNNR11O (IM21) + $C_3H_{8\,(g)}$ → BNNR11O- C_3H_8 (IM22)	-0.13	-	
(R25) BNNR11O-C_3H_8 (IM22) → BNNR11O-C_3H_7-H (IM23)	-1.26	0.82	842
(R26) BNNR11O-C_3H_7-H (IM23) → BNNR11O-2H-C_3H_6 (IM24)	0.47	1.20	1335
(R27) BNNR11O-2H-C_3H_6 (IM24) → BNNR11O-2H (IM25) + $C_3H_{6\,(g)}$	0.09	-	
(R28) BNNR11O-2H (IM25) → BNNR10O-H_2O (IM26)	1.34	1.61	872
(R29) BNNR10O-H_2O (IM26) → BNNR10O (IM27) + $H_2O_{\,(g)}$	0.20	-	

(R30) BNNR10O (IM27) + $O_{2\,(g)}$ → BNNR10O-O_2 (IM28)	-0.61	-	
(R31) BNNR10O-O_2 (IM28) → BNNR12O (IM14)	-3.33	0.13	509
(R32) BNNR12O (IM14) + $O_{2\,(g)}$ → BNNR12O-O_2 (IM15′)	0.62	-	
(R33) BNNR12O-O_2 (IM15′) → BNNR14O (IM0)	-2.26	0.67	472

Table S8: Forward rate constants (k_{for}) and equilibrium constants (K) calculated at different temperatures for the elementary steps considered in the overall reaction network of the ODHP reaction based on single point PBE-D3 corrected PBE optimized structures and free energies ($P_{C_3H_8}$ = 0.3 atm and P_{O_2} = 0.15 atm).

Reaction	T= 748 K		T = 798 K		T = 823 K	
	k_{for} (s^{-1})	K	k_{for} (s^{-1})	K	k_{for} (s^{-1})	K
R1	3.03×10^{9}	5.51×10^{-7}	2.94×10^{9}	6.93×10^{-7}	2.89×10^{9}	7.77×10^{-7}
R2	2.80×10^{6}	1.39×10^{7}	6.76×10^{6}	3.41×10^{6}	1.01×10^{7}	1.80×10^{6}
R3	2.45×10^{4}	7.26×10^{-2}	1.01×10^{5}	1.20×10^{-1}	1.92×10^{5}	1.51×10^{-1}
R4	4.54×10^{15}	1.46×10^{6}	3.33×10^{15}	1.11×10^{6}	2.87×10^{15}	9.70×10^{5}
R5	2.04×10^{-1}	1.85×10^{-6}	1.54	4.57×10^{-6}	3.85	6.89×10^{-6}
R6	1.71×10^{6}	9.73×10^{2}	4.44×10^{6}	5.87×10^{2}	6.86×10^{6}	4.66×10^{2}
R7	2.09×10^{17}	4.42×10^{7}	1.90×10^{17}	4.14×10^{7}	1.80×10^{17}	3.98×10^{7}
R8	3.03×10^{9}	6.14×10^{-7}	2.94×10^{9}	7.71×10^{-7}	2.89×10^{9}	8.63×10^{-7}
R9	2.56×10^{6}	1.63×10^{7}	6.33×106	4.04×10^{6}	9.57×10^{6}	2.14×10^{6}
R10	8.24×10^{3}	2.32×10^{-2}	3.58×10^{4}	4.04×10^{-2}	6.98×10^{4}	5.21×10^{-2}
R11	5.54×10^{15}	1.78×10^{6}	4.06×10^{15}	1.35×10^{6}	3.50×10^{15}	1.18×10^{6}
R12	2.60	1.21×10^{-6}	1.67×10^{1}	2.89×10^{-6}	3.89×10^{1}	4.28×10^{-6}
R13	6.58×10^{7}	7.92×10^{7}	1.69×10^{8}	4.69×10^{7}	2.61×10^{8}	3.70×10^{7}
R14	2.73×10^{13}	5.75×10^{3}	2.39×10^{13}	5.20×10^{3}	2.23×10^{13}	4.93×10^{3}
R15	3.03×10^{9}	5.46×10^{-7}	2.94×10^{9}	6.91×10^{-7}	2.89×10^{9}	7.75×10^{-7}
R16	3.24×10^{6}	9.16×10^{6}	7.88×10^{6}	2.29×10^{6}	1.18×10^{7}	1.22×10^{6}
R17	1.19×10^{4}	2.74×10^{-2}	5.08×10^{4}	4.86×10^{-2}	9.85×10^{4}	6.32×10^{-2}
R18	4.82×10^{15}	1.55×10^{6}	3.53×10^{15}	1.18×10^{6}	3.04×10^{15}	1.03×10^{6}
R19	1.12×10^{2}	1.21×10^{-6}	6.24×10^{2}	2.97×10^{-6}	1.36×10^{3}	4.47×10^{-6}
R20	2.34×10^{6}	8.55×10^{-4}	7.16×10^{6}	1.85×10^{-3}	1.19×10^{7}	2.64×10^{-3}
R21	6.70×10^{16}	1.41×10^{7}	4.81×10^{16}	1.05×10^{7}	4.10×10^{16}	9.06×10^{6}
R22	1.78×10^{9}	2.51×10^{-3}	1.72×10^{9}	2.03×10^{-3}	1.69×10^{9}	1.85×10^{-3}
R23	6.75×10^{5}	1.01×10^{12}	1.11×106	1.05×10^{11}	1.40×10^{6}	3.73×10^{10}

R24	3.03×10^{9}	6.58×10^{-7}	2.94×10^{9}	8.37×10^{-7}	2.89×10^{9}	9.42×10^{-7}
R25	4.09×10^{6}	1.04×10^{6}	9.59×10^{6}	2.90×10^{5}	1.41×10^{7}	1.62×10^{5}
R26	2.08×10^{5}	5.38×10^{-2}	7.33×10^{5}	9.23×10^{-2}	1.30×10^{6}	1.18×10^{-1}
R27	4.60×10^{15}	1.48×10^{6}	3.37×10^{15}	1.12×10^{6}	2.90×10^{15}	9.81×10^{5}
R28	5.71×10^{2}	1.49×10^{-7}	2.94×10^{3}	5.98×10^{-7}	6.21×10^{3}	1.12×10^{-6}
R29	9.65×10^{14}	2.04×10^{5}	8.37×10^{14}	1.82×10^{5}	7.78×10^{14}	1.72×10^{5}
R30	1.78×10^{9}	1.11×10^{-2}	1.72×10^{9}	8.32×10^{-3}	1.69×10^{9}	7.35×10^{-3}
R31	4.53×10^{8}	3.16×10^{19}	4.88×10^{8}	1.12×10^{18}	5.04×10^{8}	2.44×10^{17}
R32	1.78×10^{9}	4.49×10^{-11}	1.72×10^{9}	1.11×10^{-10}	1.69×10^{9}	1.69×10^{-10}
R33	2.59×10^{5}	2.71×10^{12}	4.83×10^{5}	2.84×10^{11}	6.41×10^{5}	1.02×10^{11}

Table S9: Surface coverage/probability density (θ) of various intermediates calculated at different temperatures for overall pathway of the ODHP reaction form a microkinetic model based on single point PBE-D3 corrected PBE optimized structures and free energies (P_{C3H8}= 0.3, and P_{O2}= 0.15 atm).

Intermediate		Surface Coverage (θ)		
		748 K	**798 K**	**823 K**
BNNR14O	(IM0)	2.23×10^{-6}	4.07×10^{-6}	5.47×10^{-6}
BNNR14O-C_3H_8	(IM1)	1.23×10^{-12}	2.82×10^{-12}	4.25×10^{-12}
BNNR14O-C_3H_7-H	(IM2)	3.47×10^{-10}	3.17×10^{-10}	3.29×10^{-10}
BNNR14O-2H-C_3H_6	(IM3)	1.50×10-^{11}	1.53×10^{-11}	1.59×10^{-1}1
BNNR14O-2H	(IM4)	2.19×10^{-5}	1.70×10^{-5}	1.54×10^{-5}
BNNR14O-2Hr	(IM5)	9.39×10^{-12}	2.09×10^{-11}	2.94×10^{-11}
BNNR13O-H_2O	(IM6)	7.18×10^{-9}	9.74×10^{-9}	1.08×10^{-8}
BNNR13O	(IM7)	3.17×10^{-1}	4.03×10^{-1}	4.31×10^{-1}
BNNR13O-C_3H_8	(IM8)	1.95×10^{-7}	3.11×10^{-7}	3.72×10^{-7}
BNNR13O-C_3H_7-H	(IM9)	6.53×10^{-5}	5.72×10^{-5}	5.25×10^{-5}
BNNR13O-2H-C_3H_6	(IM10)	1.11×10^{-7}	9.01×10^{-8}	7.99×10^{-8}
BNNR13O-2H	(IM11)	1.98×10^{-1}	1.22×10^{-1}	9.46×10^{-2}
BNNR13O-2Hr	(IM12)	7.57×10^{-9}	1.16×10^{-8}	1.36×10^{-8}
BNNR12O-H_2O	(IM13)	4.91×10^{-5}	6.97×10^{-5}	7.92×10^{-5}
BNNR12O	(IM14)	2.82×10^{-1}	3.63×10^{-1}	3.90×10^{-1}
BNNR12O-C_3H_8	(IM15)	1.54×10^{-7}	2.51×10^{-7}	3.02×10^{-7}
BNNR12O-C_3H_7-H	(IM16)	4.68×10^{-5}	4.08×10^{-5}	3.76×10^{-5}
BNNR12O-2H-C_3H_6	(IM17)	1.30×10^{-7}	9.46×10^{-8}	8.05×10^{-8}
BNNR12O-2H	(IM18)	2.02×10^{-1}	1.11×10^{-1}	8.27×10^{-2}
BNNR12O-2Hr	(IM19)	2.38×10^{-7}	3.21×10^{-7}	3.58×10^{-7}
BNNR11O-H_2O	(IM20)	2.08×10^{-11}	8.32×10^{-11}	1.52×10^{-10}
BNNR11O	(IM21)	2.94×10^{-4}	8.71×10^{-4}	1.37×10^{-3}

BNNR11O-O_2	(IM22′)	7.38×10^{-7}	1.77×10^{-6}	2.55×10^{-6}
BNNR11O-C_3H_8	(IM22)	1.93×10^{-10}	7.29×10^{-10}	1.29×10^{-9}
BNNR11O-C_3H_7-H	(IM23)	3.81×10^{-9}	9.56×10^{-9}	1.41×10^{-8}
BNNR11O-2H-C_3H_6	(IM24)	9.37×10^{-13}	2.13×10^{-12}	3.03×10^{-12}
BNNR11O-2H	(IM25)	1.39×10^{-6}	2.39×10^{-6}	2.97×10^{-6}
BNNR10O-H_2O	(IM26)	7.73×10^{-16}	9.48×10^{-15}	2.88×10^{-14}
BNNR10O	(IM27)	1.57×10^{-10}	1.73×10^{-9}	4.95×10^{-9}
BNNR10O-O_2	(IM28)	1.74×10^{-12}	1.43×10^{-11}	3.63×10^{-11}
BNNR12O-O_2	(IM15′)	1.27×10^{-11}	4.04×10^{-11}	6.61×10^{-11}

Table S10: The turnover frequency (TOF), apparent activation energy (E_{app}), and reaction orders calculated from a microkinetic reactor analysis of the proposed overall ODHP reaction based on single point PBE-D3 corrected PBE optimized structures and free energies.

Reaction pathway	**TOF (s^{-1})**			**E_{app} (eV)**	**Rate-limiting step**	**Reaction order (T= 798 K)**	
	748 K	**798 K**	**823 K**			**C_3H_8**	**O_2**
Overall reaction	5.0×10^{-1}	2.0	3.6	1.42	1st C-H cleavage of C_3H_8 on the catalyst	0.9	0.0
Path I: 14O to 12O cycle	3.4×10^{-6}	1.9×10^{-5}	4.3×10^{-5}				
Path II: 13O to 11O cycle	5.0×10^{-1}	2.0	3.6				
Path III: 12O to 10O cycle	7.9×10^{-4}	7.0×10^{-3}	1.8×10^{-2}				